Image Segmentation for Lung Region in Chest X-ray Images using Edge Detection and Morphology

Mohd Nizam Saad
School of Multimedia Technology & Communication, Universiti Utara Malaysia, Sintok Kedah, Malaysia
nizam@uum.edu.my

Zurina Muda
Faculty of Information Science & Technology, Universiti Kebangsaan Malaysia, Bangi, Selangor, Malaysia
zurina@ftsm.ukm.my

Noraidah Sahari@ Ashaari
Faculty of Information Science and Technology, Universiti Kebangsaan Malaysia, Bangi, Selangor, Malaysia
nsa@ftsm.ukm.my

Hamzaini Abdul Hamid
Radiology Department, National University Medical Center Malaysia, Bandar Tun Razak, Kuala Lumpur, Malaysia
drzanid@yahoo.com

***Abstract*—Studies of medical image segmentation have long been done as a mean to distinguish object region from one to another for further image analysis. The segmentation of lung region in chest X-ray (CXR) based on object edge detection is one of the popular method applied. Early edge detection algorithms like Sobel, Prewitt and Laplacian have been used to segment the lung however, none of them can successfully generate a truly satisfied segmentation output. The reason for this fail is because they are high pass filter that is sensitive to image noise. Hence, the requirement for better edge detection algorithm that can cope with reasonable lower and upper threshold value for image noise like canny edge should be highlighted. Moreover, combining this algorithm with morphology method (dilation and erosion) will produce better outcome. Therefore, this paper has proposed method for segmenting lung region in CXR images using canny edge filter and morphology. Although the filter can detect the lung edge, unfortunately, the final edges lines produce are still unsatisfied. To solve the problem, Euler number method is applied to extract the lung region before executing the edge detection using the filter. The implementation produced convincing result as most of the segmented image is almost similar to the ground truth image.**

***Index Terms* — Image segmentation, chest x-ray image, canny edge filter, morphology method, Euler number**

I. INTRODUCTION

According to the Ministry of Health Malaysia (2010), at the end of 2010 (the last year for Ninth Malaysia Plan), there were 178 clinics run radiology services with a total number of 415,734 chest X-ray routine performed in this country. The number is expected to increase as the country is rapidly grown with many excellent plans such as the Malaysia Plan. The increment is identical as Chest X-ray (CXR) comprises at least one-third of all diagnostic radiographic procedures and provides sufficient pathological information about cardiac size, pneumonia-shadow, and mass-lesions, with low cost and high reproducibility [2]. The numerous number of image availability has invited many researchers to conduct studies related to the image such as image segmentation.

Image segmentation is a systematic task of distinguishing objects within an image into separate regions based on certain homogeneity measurement inside a single region. Meanwhile in the field of medical image analysis, segmentation is used to delineate specific anatomical structures with the aim to diagnose various disorders, locate pathologies, create statistical atlases, quantify structural properties, etc [3]. Regardless the type of medical images used, image segmentation is mostly done at the early stage in the image processing cycle before further analysis is carried to the identified regions [4]. The application of image segmentation for the CXR images normally involved two common anatomies that are the lung and rib cage [5]. However, there are also reports on segmenting other anatomy structures in the same image type like heart, clavicles and blood vessels but they are not as aggressive as the duo. In order to segment the lung anatomy into separate regions, there are three features that are commonly used which include texture feature, geometric feature and contrast feature [6].

The lung segmentation based on geometric feature like object edge, circularity and image size has long been introduced to isolate the lung region from other anatomies inside the CXR image. Segmenting the lung with edge detection is fundamental and essential in pre-processing step because edges represent important contour features within the corresponding image [7]. Although early brought edge detection algorithms like Sobel, Prewitt and Laplacian have been used to segment objects for medical image, however in theory, they belong to the high pass filtering, which are not fit for noise in medical image edge detection [8]. Moreover, in real world applications, medical images contain complex object boundaries, shadows and noises which result difficulties to distinguish their exact edge from noise or trivial geometric features [9]. While the mentioned algorithms can only detect edges within little or probably no noise existence, the edge detection for segmenting lung region with these algorithms would be very sensitive and resulting unbearable outcome. If these algorithms are solely used for edge detection in lung segmentation, it also might cause large amount of calculation and it is expected that they cannot meet real-time requirement in many places [10]. Therefore, segmenting lung region within the CXR image based on edge detection must come with additional technique such as morphology which is more robust to noise so that segmentation output can become better.

978-1-4799-5686-9/14/$31.00 ©2014 IEEE

Realizing the importance of this additional technique, this paper is written. It is a mean of sharing our experience in segmenting the lung region in CXR images using canny edge detection along with morphology technique which has shown quite effective combination to do the segmentation. Hence, to ease the knowledge sharing the paper is outlines as follow: segmentation method is discussed in Section II, Section III presents the image dataset, Section IV provides details explanation on the experiment, information regarding the evaluation is provided in Section V, while Section VI presents the discussion and later concludes our work in this paper.

II. Segmentation Method

The proposed solution to segment the lung from the CXR images was based on the shape of the lung. In order to decompose the region, canny operator is used as the edge detection algorithm to detect the structure of the lung shape. This edge detection algorithm serves to simplify the analysis of images by drastically reducing the amount of data to be processed, at the same time preserving useful structural information about object boundaries [11]. Once the edge detection completed, we followed further steps from [8] and [12] where they have applied morphology method namely dilation to grow the edge so that it covers the interest anatomy region. An accurate dilation value must be estimated so that the growing process does not exceed the interest region. As a step of precaution, any unwanted growing region will be eliminated so that the leftover is only the targeted region. To do the elimination, another morphology technique; erosion is applied. The reduction will shrink the targeted region hence only the lung region is segment. The whole segmentation processes contained six tasks which can be overviewed in Fig.1.

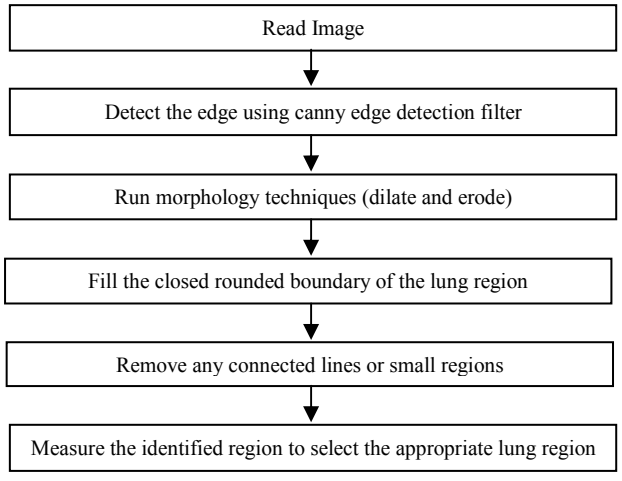

Fig.1. Six tasks of the segmentation process

In the first task; read image, selection of CXR images are made from the dataset which in our case, we used Japan Society of Radiological Technology (JSRT) image dataset (section III will elaborate in details about this dataset). The original image is quite huge (2048x2048) hence it need to be resized in manageable size of 600x600 resolutions. The other reason for this image size reduction is done is to prevent the matrix size of the image for being too large.

The second tasks tend to discriminate between the image foreground and background and turn them into a binary image using canny edge filter. However, the most important aim for running this task is to get the edge for all objects located inside the image especially the lung region.

The third task is to improve the edge derived after executing the edge detection via canny edge filter. This task occupies morphology method which involved dilation and erosion. The basic operation of dilation and erosion can be formulated as follow (F is regarded as image set, S is regarded as structure element):

Dilation operation can be defined as:

$$F \oplus S\ (m,n) = \max\{F(m-x,n-y) + S(x,y)\} \quad (1)$$

Meanwhile the erosion operation can be defined as:

$$F \oplus S\ (m,n) = \min\{F(m+x,n+y) - S(x,y)\} \quad (2)$$

Dilation is an expansive process that makes the target grown and the hole contracted while capable to combine background points around the image and connect two adjacent objects [10]. Conversely, erosion is a contractive process that makes the target contracted and the hole expanded to eliminate useless point and separate two small connected objects. In our segmentation method, dilation and erosion are used because canny edge filter cannot detect the actual object edge perfectly as expected since the existence of noise. Hence, dilation will reconnect the unconnected dotted edge line especially those that form the region shape. Afterwards, the erosion will remove the unwanted edge line connected to the targeted region.

The fourth task filled the closed rounded boundary once the edge of the lung region is formed as a closed rounded line. The region area can be filled so that it can become the region of interests (ROI) which are presented in the form of binary large object (BLOB). The ROI is important because soon after, it will become the image mask for the other detection tasks.

The removal task is carried out in order to detach each ROI with its adjacent region so that they will exist as a single unit object. If this task is ignored, there might be possibility that the targeted lung region will include other unwanted regions especially those small regions neighbor located close to the lung.

Finally, the measurement task is done to calculate the two biggest regions shown in the image. Since the fourth task produced small regions apart from the lung shape needed, these regions must be deleted. In the case of lung shape inside the CXR image, normally the biggest region is the right lung while the second biggest is the left lung. Hence, combining these two regions will produce the overall lung shape.

III. IMAGE DATASET

The CXR images used to test the technique were taken from a public chest radiograph database of Japan Society of Radiological Technology (JSRT) at http://www.jsrt.or.jp/jsrt-db/eng.php [13]. One should become an authenticated user of the website before being allowed to download these images. There are 247 CXR images available in the database which is clustered into two parts. The first part contains CXR images with nodule and there are 154 image files in this part. On the other hand, the second part contains images without nodule with 93 image files. These images were scanned from films and have standard size of 2048 x 2048 pixels. Meanwhile, the wide density range for these images was 12 bit gray levels with 4096 grayscale. Since the JSRT only uploaded these images in the form of raw files (.iso format), we have to use additional image file viewer to open and save it into the desired format. To complete the task, JSRT recommended the usage of Image J; an open source image file viewer. Hence in our case, we use Image J to open and save the file in Bitmap format (.bmp). Although DICOM is mostly preferable format in medical imaging [13][14], we use Bitmap because it has the capability to maintain the original appearance without compressing image pixels.

Apart from the image files, JSRT also provided text file (.txt) as a mean for additional information regarding the images which contain patient age, gender, diagnosis and detected location of the anomalies. Fig. 2 shows an example of CXR image with nodule taken from JSRT database.

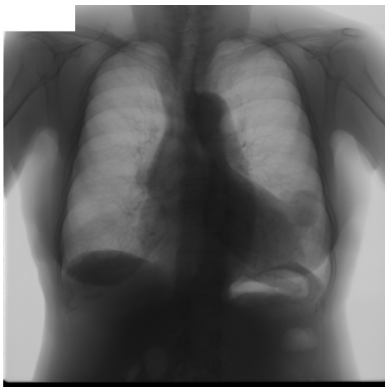

Fig. 2. A CXR image with nodule taken from JSRT database

IV. EXPERIMENT

Based on the method described in Section II, we implemented the CXR image segmentation for selected images from the JSRT dataset. The image segmentation system is developed using Matlab 2012a equipped with Image Processing Toolbox. A total of 10 images; formatted as portable network graphic (.PNG) file, were segmented as a mean to test the system capability. The grayscale level of these image files were downsized from 12 bit gray levels with 4096 grayscale to 8 bit with 256 grayscale. At the end of the segmentation process, the image outcomes were saved the same image format as its input.

When the system was first executed, one major problem identified which appeared to be the output of binary image from the second task; edge detection. Surprisingly, the object edge detected contains lots of edge line that does not represent the lung shape. Fig. 3A shows the original image and Fig. 3B shows the edge detected from the second task.

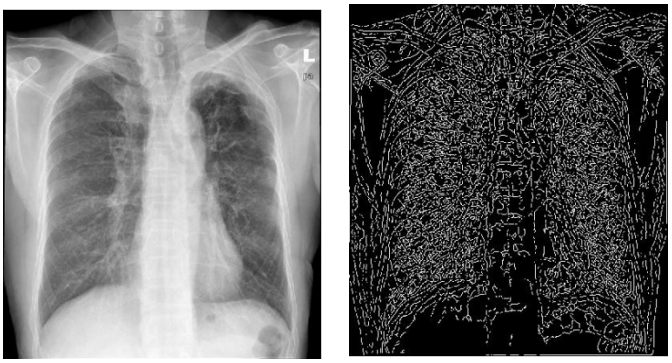

(A) (B)

Fig. 3. (A) the original image and (B) the edge detected

When the edge is presented as the image in Fig. 3B, it would be very difficult to form the actual lung shape because the existence of too many lung edges. The problem appeared because the canny edge filter used might not have the capability to filter noise in the form of tiny marginal different of gray color in the image. This has lead to difficulties choosing the upper and lower threshold value for the canny edge filter. After all, the trial and error method of guessing the threshold values are time consuming and not feasible for processing mass number of x-ray images.

In order to solve the edge detection problem, especially those relates to finding suitable threshold value, we adapted work by [16] on Euler number method before implementing edge detection. In this method, Euler number is used to extract the lung region in CXR image. The method is based the image connectivity and holes of in an X-ray image. According to them, the fundamental relationship between the number of connected object components, C and the number of object holes H in an image is called Euler number and it is defined as $E=C-H$. Number of connected object components and object holes could be calculated by local neighborhood computation. Bit quad (set of 2x2 pixels) counting provides a very simple means of determining the Euler number of an image. The Euler number can be computed as:

$$E=\frac{1}{4}\left\{n(Q1)-n(Q3)+2n\{Qd\}\right\} \quad (3)$$

Applying the Euler number method enables the pixels in lung region to be connected separating them with the unwanted neighboring area recognized as the objects holes. For further understanding on how the method works, readers are recommended to refer to [16]. Fig. 4 shows the binary image after applying the Euler method.

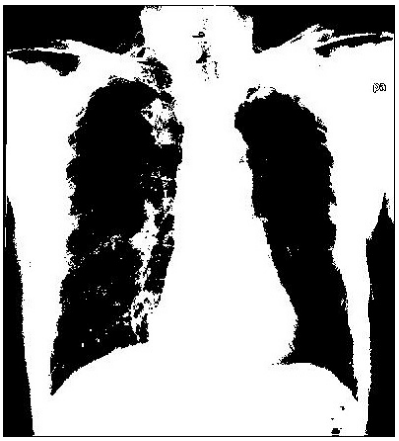

Fig. 4. Binary image after applying Euler method

Soon after applying the Euler number method, the edge detection task is executed to the binary image as shown in Fig.4. The edge detection is easy then since no additional effort required to guess the high and low threshold value for the canny edge filter as what remains is only white and black pixels (before the Euler method, the image pixels exist in gray color). Fig. 5 shows the image outcome of the lung region edge after the edge detection completed. The edge is more meaningful although some lines are not fully interconnected.

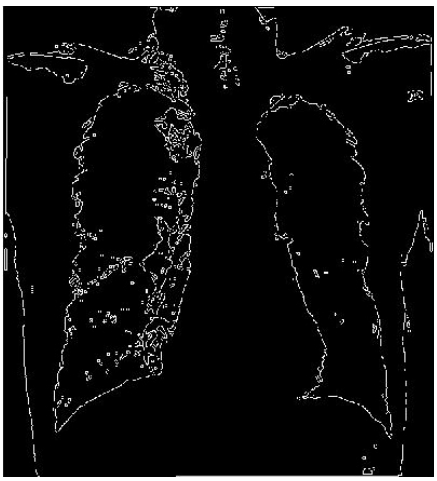

Fig. 5. Lung region edge after the edge detection

Once the lung edge is formed, it automatically produced a region with closed rounded boundary that separates it from other regions. The region is filled together to generate image BLOB and later known as the ROI. The ROI will become an image mask to the original image. Afterward, any connected lines and small regions that still attached to the ROI will be removed. The removal task cleans up the ROI from unwanted lines and regions. The outcome from this fourth and fifth task is an image with two ROIs namely left and right lung as depicted in Fig. 6.

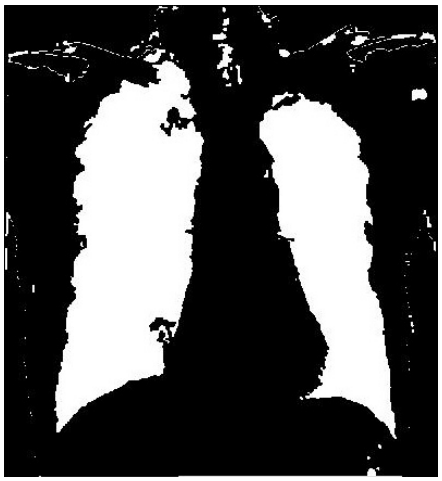

Fig. 6. Two ROIs that formed the left and right lung

V. EVALUATION

To evaluate the similarity of the segmented lung created from the chest X-ray image, a similarity measurement test is applied between the segmented lung region and the actual lung region within the image. The segmented region is derived based on the segmentation tasks done to 10 selected images in the dataset. These images and their segmentation result can be accessed via *http://www.4shared.com/rar/Vnd2LkRFce/SegmentedCXR.html*. Meanwhile, the actual lung region called as the ground truth (GT) is derived by applying manual region tracing on the lung area using proprietary graphic application; Adobe Photoshop. In order to do the manual tracing, we move the magnetic lasso tool (a tool that is available in Photoshop) carefully along the lung shape contour to get the actual shape. Once the tracing task completed, the selected area is highlighted and colored while the other unrelated is dimmed. Soon after, this GT file will be saved as a portable network graphic file format. Fig. 7 shows the GT6 for Image 6 after the tracing task.

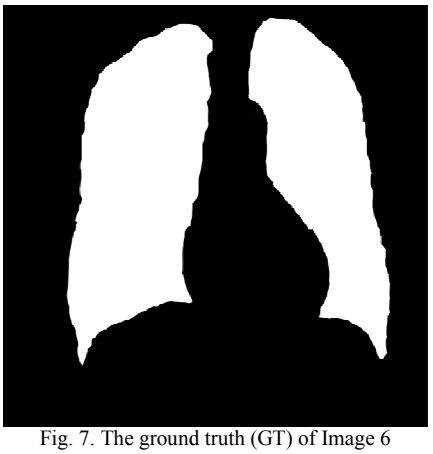

Fig. 7. The ground truth (GT) of Image 6

The similarity measurement is computed using Jaccard Similarity Coefficient for overlap measurement between the two regions. This technique is adapted based on the work done

by [17]. According to them, the Jaccard Similarity Coefficient is the agreement between GT and the estimated segmentation mask (S) over all pixels in the image. The Jaccard Similarity Coefficient can be formulated it as follows:

$$\Omega = \frac{|S \cap GT|}{|S \cup GT|} = \frac{|TP|}{|FP| + |TP| + |FN|} \quad (4)$$

where TP (true positives) represents correctly classified pixels, FP (false positives) represents pixels that are classified as object but that are in fact background, and FN (false negatives) represents pixels that are classified as background but that are in fact part of the object. The derived values for similarity measurement between each image and the GT using the Jaccard Similarity Coefficient are listed in Table I. The table listed the coefficient value according to the overall lung shape (labeled as All Lung), the right lung and the left lung. Meanwhile Table II revealed the average score for each coefficient value for all types of lung images.

TABLE I. JACCARD SIMILARITY COEFFICIENT VALUE FOR 10 SEGMENTED IMAGES

Image	Jaccard Similarity Coefficient Value		
	All Lung	Right Lung	Left Lung
1	0.799	0.799	0.819
2	0.738	0.731	0.756
3	0.808	0.825	0.795
4	0.880	0.920	0.837
5	0.826	0.863	0.780
6	0.833	0.832	0.847
7	0.823	0.823	0.822
8	0.819	0.877	0.746
9	0.769	0.783	0.763
10	0.798	0.841	0.730

TABLE II. AVERAGE SCORE FOR EACH JACCARD SIMILARITY COEFFICIENT VALUE

	All Lung	Right Lung	Left Lung
Average Score	0.809	0.829	0.790

According to [17], the Jaccard Similarity Coefficient value can be interpreted with simple explanation where the higher the value derived means the closer the image mask comparable to the GT image. Conversely, the lower value means the lesser the image mask alike to the GT. Hence, based on the coefficient values in Table 1, we can indicated that all scores are relatively high with above 0.7 out of 1 (for exact similarity). The highest similarity score is Image 4 for Right Lung (0.920) while the lowest score is Image 10 for Left Lung (0.730). In addition to the values listed in Table I, the average similarity score (depicted in Table II) for each lung's image masks as compared to the GT is also moderately high with All Lung scores 0.809, Right Lung gets 0.829 and Left Lung obtains the lowest with 0.790. These results revealed that the proposed segmentation method is helpful to segment the lung region from the CXR images for further image analysis. As described in the experiment section, it is very straightforward method, yet the outcome is still convincing.

VI. DISCUSSION AND CONCLUSION

There are a lot of papers reported good segmentation results for CXR images. In fact, for the JSRT image dataset itself, we found that many researchers claimed that the result is much higher as those obtained in this paper. For instance in [17], the average similarity score for JSRT image dataset based on Jaccard Similarity Coefficient is 0.954, 0.951 and 0.957 for All Lung, Right Lung and Left Lung respectively (refer Table II in [17]). Meanwhile, in [18], the segmentation results gathered for all lung region after applying a special technique called 'Gold Standard' are 0.93 for Active Shape Method (ASM), 0.95 for Shape Fit Mode (SFM) and 0.93 for Active Appearance Model (AAM) (refer Table 4 in [18]). The two examples show that the similarity results for lung region segmentation are extremely higher that what we achieved. Here, we revealed at least two improvements that need to be taken for the proposed method. First, the method should be robust to image noise especially those relate to grayscale image. In this experiment, we struggled to get the acceptable low and high threshold value for the canny edge detection which later required us to use the Euler number to ease the detection process. Hence, for future improvement, additional method like occupying machine learning method to learn image's visual features should be considered. Secondly, our unsupervised segmentation method is still unable to recognize the lung region correctly whereas this can be improved by using supervised method. As reported in [18], all their supervised segmentation methods; ASM, SFM and AAM have indicated high segmentation results. The situation occurred because these methods will mark the lung region manually using certain points before the marked points are saved and later used to train the algorithm to recognize the shape of the lung region. Of course, the drawback of these methods is that it is tedious job especially when the amount of image is huge. Therefore, to improve the proposed method, hybrid method can be considered by combining the unsupervised and supervised segmentation method.

As conclusion, in the paper, we have shared or experience on segmenting the lung shape on CXR image. The segmentation process starts by detecting the lung edge using canny edge detection filters. To improve the edge detection, Euler number method is applied. Later, morphology method is used to make the lung edge better so that the final output of lung region can be generated. After implementing the segmentation task, the output in the form of lung region mask is compared to the GT image to check their similarity. In the evaluation, the Jaccard Similarity Coefficient is used to calculate the similarity. The value derived from the test is moderately high although it cannot exceed other prior researchers score. In the future, the proposed segmentation method can be modified to be applied to other medical image

types such the MRI and CT so that the ROI can be isolated from the other parts.

ACKNOWLEDGMENT

This study was supported by the Geran Universiti Penyelidikan, Universiti Kebangsaan Malaysia (UKM) code GUP-2012-011. Additionally, the first author would like to thank Dr. Afzan Adam and Dr. Azizi Abdullah from the Faculty of Information Science and Technology, UKM, Malaysia for providing good comments and recommendation to improve the segmentation method as well as the system developed.

REFERENCES

[1] Kementerian Kesihatan Malaysia, "Annual Report 2010: Ministry of Health," 2010.

[2] Y. Tao, Z. Peng, A. Krishnan, and X. S. Zhou, "Robust learning-based parsing and annotation of medical radiographs.," *IEEE Trans. Med. Imaging*, vol. 30, no. 2, pp. 338–50, Feb. 2011.

[3] B. Ibragimov, B. Likar, F. Pernuš, and T. Vrtovec, "A game-theoretic framework for landmark-based image segmentation," *IEEE Trans. Med. Imaging*, vol. 31, no. 9, pp. 1761–1776, 2012.

[4] P. M. Ferreira, T. Mendonça, J. Rozeira, and P. Rocha, "An annotation tool for dermoscopic image segmentation," in *Proceedings of the 1st International Workshop on Visual Interfaces for Ground Truth Collection in Computer Vision Applications - VIGTA '12*, 2012, pp. 1–6.

[5] B. van Ginneken, B. M. ter Haar Romeny, and M. A. Viergever, "Computer-aided diagnosis in chest radiography: a survey.," *IEEE Trans. Med. Imaging*, vol. 20, no. 12, pp. 1228–41, Dec. 2001.

[6] D. Ben Hassen and H. Taleb, "Lesion detection in lung regions that are segmented using spatial relations," in *International Conference on Information Technology and e-Services*, 2012, pp. 1–4.

[7] J. Jiang, C. Chuang, Y. Lu, and C. Fahn, "Mathematical-morphology-based edge detectors for detection of thin edges in low-contrast regions," *IET Image Process.*, vol. 1, no. 3, pp. 269–277, 2007.

[8] Z. Yu-Qian, G. Wei-Hua, C. Zhen-Cheng, T. Jing-Tian, and L. Ling-Yun, "Medical images edge detection based on mathematical morphology," in *Proceedings of the IEEE Engineering in Medicine and Biology 27th Annual Conference*, 2005, vol. 6, pp. 6492–5.

[9] P. Suapang, C. Naruephai, M. Thongyoun, and S. Chivaprecha, "Mammographic masses segmentation based on morphology," *5th Biomed. Eng. Int. Conf.*, pp. 1–4, Dec. 2012.

[10] H. Huang, H. Wang, F. Guo, and J. Zhang, "A Gray-scale Image Edge Detection Algorithm Based on Mathematical Morphology," in *Third International Conference on Measuring Technology and Mechatronics Automation*, 2011, pp. 62–65.

[11] J. Canny, "A computational approach to edge detection.," *IEEE Trans. Pattern Anal. Mach. Intell.*, vol. 8, no. 6, pp. 679–98, Jun. 1986.

[12] W. Bingrong and X. Mei, "An Interactive Segmentation of Medical Image Series," *2008 Int. Semin. Futur. Biomed. Inf. Eng.*, vol. 2, no. 1, pp. 7–10, Dec. 2008.

[13] J. Shiraishi, S. Katsuragawa, J. Ikezoe, T. Matsumoto, T. Kobayashi, K. Komatsu, M. Matsui, H. Fujita, Y. Kodera, and K. Doi, "Development of a digital image database for chest radiographs with and without a lung nodule: Receiver operating characteristic analysis of radiologists' detection of pulmonary nodules," *Am. J. Roentgenol.*, vol. 174, no. 1, pp. 71–74, 2000.

[14] A. P. Bhagat and M. Atique, "Medical images: Formats, compression techniques and DICOM image retrieval a survey," in *Devices, Circuits and Systems (ICDCS), 2012 International Conference on*, 2012, pp. 172–176.

[15] P. Suapang and K. Dejhan, "Medical Image Compression and DICOM-Format Image Archive," in *IInternational Joint Conference CROS-SICE*, 2009, pp. 1945–1949.

[16] L. P. Wong and H. T. Ewe, "A Study of Lung Cancer Detection using Chest," in *3rd APT Telemedicine Workshop 2005*, 2005, pp. 210–214.

[17] S. Candemir, S. Jaeger, K. Palaniappan, J. P. Musco, R. K. Singh, Zhiyun Xue, A. Karargyris, S. Antani, G. Thoma, and C. J. McDonald, "Lung segmentation in chest radiographs using anatomical atlases with nonrigid registration.," *IEEE Trans. Med. Imaging*, vol. 33, no. 2, pp. 577–90, Feb. 2014.

[18] B. van Ginneken, M. B. Stegmann, and M. Loog, "Segmentation of anatomical structures in chest radiographs using supervised methods: a comparative study on a public database.," *Med. Image Anal.*, vol. 10, no. 1, pp. 19–40, Mar. 2006.